Variability-induced transition in a net of neural elements: From oscillatory to excitable behavior

Erik Glatt, Martin Gassel, and Friedemann Kaiser
Institute of Applied Physics, Darmstadt University of Technology, 64289 Darmstadt, Germany
(Received 17 January 2006; published 30 June 2006)

Starting with an oscillatory net of neural elements, increasing variability induces a phase transition to excitability. This transition is explained by a systematic effect of the variability, which stabilizes the formerly unstable, spatially uniform, temporally constant solution of the net. Multiplicative noise may also influence the net in a systematic way and may thus induce a similar transition. Adding noise into the model, the interplay of noise and variability with respect to the reported transition is investigated. Finally, pattern formation in a diffusively coupled net is studied, because excitability implies the ability of pattern formation and information transmission.

DOI: 10.1103/PhysRevE.73.066230 PACS number(s): 05.40.−a, 05.70.Fh

In recent decades it was shown that noise has a strong influence on the dynamics of many nonlinear systems. Examples are stochastic resonance [1], spatiotemporal stochastic resonance [2,3], and noise-induced phase transitions [4]. A special noise-induced phase transition in a net of oscillatory FitzHugh-Nagumo (FHN) [5] elements was reported in [6] and further studied, using colored multiplicative noise, in [7]. This transition leads to the suppression of synchronous oscillations and the restoration of excitable dynamics. This phenomenon [noise-induced excitability (NIE)] is caused by a systematic contribution of parametric noise, which stabilizes a deterministically unstable fixed point of the local dynamics. In contrast to noise internal variability, which is also omnipresent in nature, denotes static stochastic differences between the otherwise equal elements of a net. Variability can influence the spatiotemporal dynamics of many systems. The influence of parameter variability on the synchronization of coupled oscillators was investigated by Winfree [8] and Kuramoto [9]. These results are the basis for most of the studies on synchronization even today [10]. The effect of variability on spatiotemporal chaos was observed in [11]. Furthermore, variability can play an important role for pattern formation in a net of biochemical oscillators [12]. Stochastic influences are also relevant in gene expression, e.g., providing the flexibility needed by cells adapting to fluctuating environments [13].

Some of these theoretical findings were confirmed by experiments and seem to play an important role in biological and chemical systems. Fluctuations are able to enhance the output signal of a neuron [14] and help the paddle fish to locate its prey [15]. Furthermore, stochastic influences can support pattern formation and wave propagation in spatially extended systems, for example, in the photosensitive Belousov-Zhabotinsky reaction [16,17].

In this paper it is shown that variability can have a systematic effect on a biophysical net, similar to the systematic contribution of multiplicative noise, which follows from small noise expansion [4]. In a large net with sufficient coupling strength this effect can induce a phase transition. To demonstrate this a net of globally coupled oscillatory FHN elements is studied, where an increasing variability leads to a transition from the oscillatory regime to the excitable one [variability-induced excitability (VIE)]. In a next step parametric noise [6,7] is added in the model equations and its interplay with the variability is investigated. Both have a strong systematic influence on the net dynamics and thus on the border between the oscillatory and the excitable regimes. Finally, pattern formation in a diffusively coupled net in the presence of both noise and variability is studied, because the occurrence of excitability allows information transmission in such a net (excitation waves). The observed pattern formation strongly depends on the variability and on the noise.

The system under consideration is a net of $N \times N$ coupled FHN elements in the presence of parametric multiplicative noise $\eta_{ij}(t)$ and variability in the parameter c,

$$\dot{u}_{ij} = \frac{1}{\epsilon}[u_{ij}(1-u_{ij})(u_{ij}-a) - v_{ij} + d_u] + q_u K_{ij},$$

$$\dot{v}_{ij} = u_{ij} - c_{ij}(1+\eta_{ij})v_{ij}, \tag{1}$$

where K_{ij} and q_u denote the coupling function and strength, respectively. In this minimal model of neural dynamics $u_{ij}(t)$ represents the fast relaxing membrane potential, while $v_{ij}(t)$ denotes the slow ion recovery variable. For a single element the set of two equations describes essential parts of the Hodgkin-Huxley model for neuronal dynamics quite well. Other minimal models are also of relevance, e.g., a direct reduction of the four-variable Hodgkin-Huxley model [18].

The time scales are separated by the small parameter $\epsilon = 0.01$. The time is specified in time units (t.u.), which accord approximately with the oscillation period of the net. The equations are integrated on a discrete spatiotemporal grid using the Heun method ($\Delta t = 0.001$ t.u.) [4] and the forward time centered space scheme ($\Delta h = 1.0$) in time and space, respectively. The integration in space is performed using periodic boundary conditions. The grid points are labeled by the indices $1 \le i, j \le N$.

In the present paper only noise and variability in the slow variables $v_{ij}(t)$ are considered. Only multiplicative parametric noise has a systematic effect on the global net dynamics and thus only noise and variability in the parameter c are studied. Due to the variability the values (c_{ij}) of the parameter c can change from element to element. The parameter values c_{ij} are Gaussian distributed numbers, with

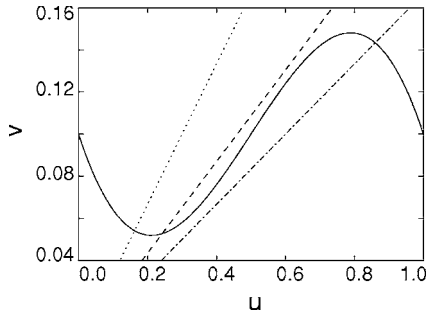

FIG. 1. Nullclines in phase space (u,v) for one FHN element [Eq. (1)]: (—) cubic nullcline, (···) linear nullcline with $c_{ij}=3.0$, (- - -) linear nullcline with $c_{ij}=4.6$, and (-·-) linear nullcline with $c_{ij}=6.0$.

$$\langle c_{ij}c_{kl}\rangle = \sigma_v^2\delta_{ij,kl}, \quad \langle c_{ij}\rangle = C. \tag{2}$$

In the following, σ_v^2, the variance of the Gaussian distribution $P(c,\sigma_v)$, denotes the variability intensity and σ_v the variability strength. The term $\eta_{ij}(t)$ is taken to be zero-mean spatially uncorrelated Gaussian white noise. Hence the correlation function reads

$$\langle \eta_{ij}(t)\,\eta_{kl}(t')\rangle = \sigma_m^2\delta_{ij,kl}\delta(t-t'), \tag{3}$$

with the noise intensity σ_m^2 and the noise strength σ_m.

Throughout this paper the following set of parameters is used: $(a,C,d_u)=(0.5,4.6,0.1)$, while the coupling strength q_u, the system size, the noise strength σ_m, and the variability strength σ_v are varied. For $\sigma_m=0$ and $\sigma_v=0$, each FHN element performs autonomous limit cycle oscillations, yielding a synchronized output in the case of $q_u>0$ and appropriate initial conditions.

The dynamics of a FHN element strongly depends on its parameter value c_{ij} (Fig. 1) and thus on the gradient angle of the linear nullcline

$$\alpha(c_{ij}) = \arctan(c_{ij}^{-1}). \tag{4}$$

For $4.41\le c_{ij}\le 5.19$ the element is in the oscillatory regime (limit cycle around an unstable fixed point). For $c_{ij}>5.19$ a stable fixed point occurs on the right side of the local maximum of the cubic nullcline and for $0\le c_{ij}<4.41$ on the left side of the local minimum of the cubic nullcline. In the last case a small excitation can stimulate a large loop in phase space (single spike) before the element goes back to the fixed point. This dynamic regime is called the excitable regime. For $c_{ij}<0$ the dynamics of the element completely changes, causing the numerical integration to get unstable. Consequently the parameter values $c_{ij}<0$ have to be excluded by setting the probability distribution $P(c,\sigma_v)$ to zero for corresponding values of c. For $\sigma_v=2.5$, the largest variability strength used in this paper, this means that 3% of the Gaussian-distributed c_{ij} are excluded. This discussion shows that the net [Eq. (1)] with variability in the parameter c consists of elements in different dynamical regimes [Fig. 2(a)], where the probability of an element to be excitable depends on σ_v [Fig. 2(b)].

First a global coupling of the net is considered. The coupling function is defined as

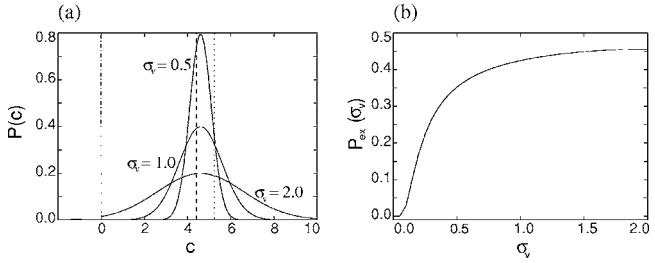

FIG. 2. (a) (—) Probability distributions $P(c,\sigma_v)$ for three different σ_v. Borders between the dynamical regimes: (···) $c=5.19$, (- - -) $c=4.41$, (-·-) $c=0$. (b) Probability $P_{ex}(\sigma_v)$ for one element to be in the excitable regime $(0\le c_{ij}<4.41)$.

$$K_{ij} = \bar{u} - u_{ij}, \tag{5}$$

where $\bar{u}$ denotes the mean value of the fast variable for all elements (mean field). Later, in order to study pattern formation and signal transmission through the array, the function K_{ij} is chosen as diffusive nearest-neighbor coupling, using a nine-point Laplacian for radial symmetry,

$$K_{ij} = \nabla^2 u_{ij},$$

$$\nabla^2 u_{ij} = \frac{1}{6}[u_{i+1,j+1} + u_{i+1,j-1} + u_{i-1,j+1} + u_{i-1,j-1} + 4(u_{i+1,j} + u_{i-1,j} + u_{i,j+1} + u_{i,j-1}) - 20u_{i,j}]. \tag{6}$$

In the following a net is called oscillatory if a spatially uniform solution, which is periodic in time, is stable. If a spatially uniform, temporally constant solution is stable and a small excitation can cause a large loop in phase space, the net is called excitable. If diffusive coupling is used one can observe patterns like scroll rings or spiral waves in an excitable net [19]. If these patterns vanish for $t\to\infty$ the net is called subexcitable [20]. In this paper these expressions are also used for finite nets with noise and variability even if in these cases small fluctuations around these ideal solutions occur.

The multiplicative noise $\eta_{ij}(t)$ may have a systematic effect on the dynamics of a FHN element and thus on the dynamics of the net [6,7]. This can be shown when a small noise expansion [4] is applied. The first order of the expansion reads

$$\dot{u}_{ij} = \frac{1}{\epsilon}[u_{ij}(1-u_{ij})(u_{ij}-a) - v_{ij} + d_u] + q_u K_{ij},$$

$$\dot{v}_{ij} = u_{ij} - c_{ij}\left(1 - \frac{1}{2}\sigma_m^2 c_{ij}\right)v_{ij}. \tag{7}$$

This result means that the parameter σ_m changes the gradient angle of the linear nullcline for all elements,

$$\alpha(c,\sigma_m) = \arctan\left[\left(c - \frac{1}{2}\sigma_m^2 c^2\right)^{-1}\right]. \tag{8}$$

Increasing the noise strength starting with $\sigma_m=0$ tilts the linear nullclines to the left. For $\sigma_v=0$ this means that the unstable fixed point of the local dynamics moves toward the

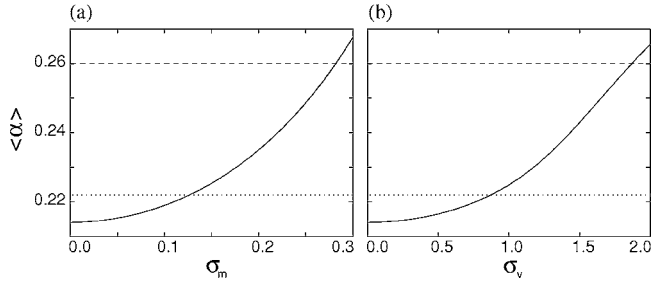

FIG. 3. Mean gradient angle $\langle\alpha\rangle$ from Eq. (10) for a large net of FHN elements [Eq. (1)], (a) dependent on σ_m with $\sigma_v=0$, (b) dependent on σ_v with $\sigma_m=0$. $(\cdots)$ $\langle\alpha\rangle=0.222$. (- - -) $\langle\alpha\rangle=0.260$.

stable branch of the cubic nullcline and becomes stable for $\sigma_m \approx 0.13$. Multiplicative noise can thus induce a transition from an oscillatory to an excitable net [6]. The variability in the parameter c does act in a different way, but it also has a systematic effect on the net. The mean gradient angle of the linear nullclines of the net,

$$\langle\alpha\rangle = \frac{\sum_{i,j=1}^{N} \alpha(c_{ij},\sigma_m)}{N^2}, \tag{9}$$

is a macroscopic net parameter. This parameter can be calculated approximately for a large net,

$$\langle\alpha\rangle \approx \langle\alpha\rangle(\sigma_m,\sigma_v) = \int_{-\infty}^{\infty} \alpha(c,\sigma_m)P(c,\sigma_v)dc. \tag{10}$$

Using Eqs. (8) and (10) one finds that $\langle\alpha\rangle$ depends on σ_v and σ_m.

The results of Eq. (10) for a system in the presence of the multiplicative noise, but without variability, are displayed in Fig. 3(a). The parameter $\langle\alpha\rangle$ is growing with increasing noise strength. For $\alpha_{ij} \gtrsim 0.222$ the fixed point of a single element is stable and thus the element is in the excitable regime. For that reason one expects a large strongly coupled net to show excitable behavior for $\sigma_m \gtrsim 0.13$. This was demonstrated in [6,7]. For $\langle\alpha\rangle \approx 0.260$ the subexcitable regime in a diffusively coupled net is reached. In Fig. 3(b) the influence of the variability strength on $\langle\alpha\rangle$ for $\sigma_m=0$ is shown. The mean gradient angle is growing with σ_v and one would expect a transition to VIE in a strongly coupled net, similar to NIE.

In Fig. 4 the mean gradient angle $\langle\alpha\rangle$ is plotted for a net in presence of the noise and the variability. The value of the mean gradient angle does strongly depend on σ_m and σ_v. If, as assumed, $\langle\alpha\rangle$ is the relevant parameter for the observed dynamics of the net one expects to find a transition from the oscillatory to the excitable regime for values of σ_m and σ_v associated with $\langle\alpha\rangle \approx 0.222$. The same is true for the transition to the subexcitable regime in a diffusive coupled net for $\langle\alpha\rangle \approx 0.260$.

To find the expected transition from an oscillatory net to a net with a stable spatially uniform temporally constant solution in simulations of Eq. (1) the time average of the mean field of the fast variable

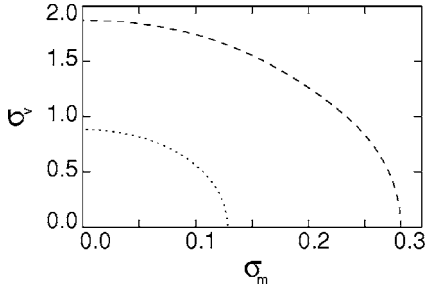

FIG. 4. Mean gradient angle $\langle\alpha\rangle$ from Eq. (10) for a large net of FHN elements [Eq. (1)], dependent on σ_v and σ_m; $(\cdots)$ $\langle\alpha\rangle=0.222$, (- - -) $\langle\alpha\rangle=0.260$.

$$M = \langle\bar{u}\rangle_t \tag{11}$$

is used as an order parameter. The transition is associated with a jump in this parameter from $M>0.40$ for an oscillatory net to $M<0.24$. In the following this jump is marked by a contour line for $M=0.25$, which is denoted by M_{fi}. To display that the net is excitable one has to show additionally that the elements of the net are in the part of phase space where an excitation is possible [6]. For that reason the relative rest time (RRT) of all elements of the net in this special part of phase space ($u_{ij}<0.35$ and $v_{ij}<0.1$) is used as an additional order parameter. The transition to excitability is marked by a contour line for the value 0.98 of the RRT. This contour line is denoted by RRT_{ex}. One has to notice here that the transition to the subexcitable regime does not cause a jump in the RRT and hence can only be measured qualitatively [7].

Numerical results for M and the RRT on varying the coupling strength q_u are plotted in Fig. 5. With the multiplicative noise and $\sigma_v=0$ one finds the expected transition from an oscillatory net to an excitable one [Figs. 5(a) and 5(b)]. M_{fi} depends on q_u and for a weak coupling ($q_u<20$) the spatially homogeneous solution of the net does not become stable. A strong coupling is necessary to minimize the random influ-

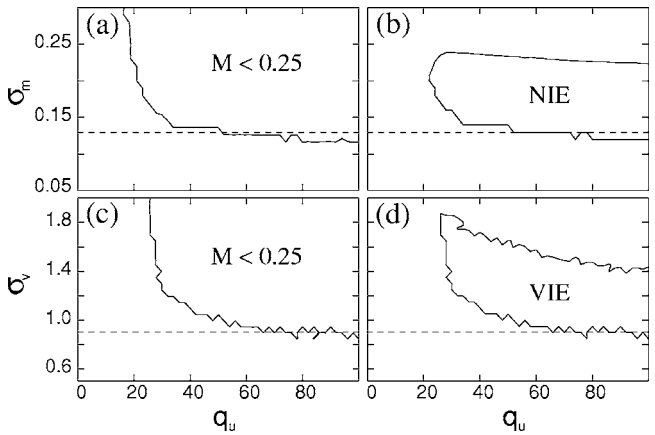

FIG. 5. Results for Eq. (1) with global coupling [Eq. (5)]. (a),(b) boundaries of NIE, $\sigma_v=0$. (c),(d) boundaries of VIE, $\sigma_m=0$. (a),(c) mean field, (—) M_{fi}. (b),(d) relative rest time, (—) RRT_{ex}. (- - -) predicted border of oscillatory and excitable nets. Other parameters: $N=100$.

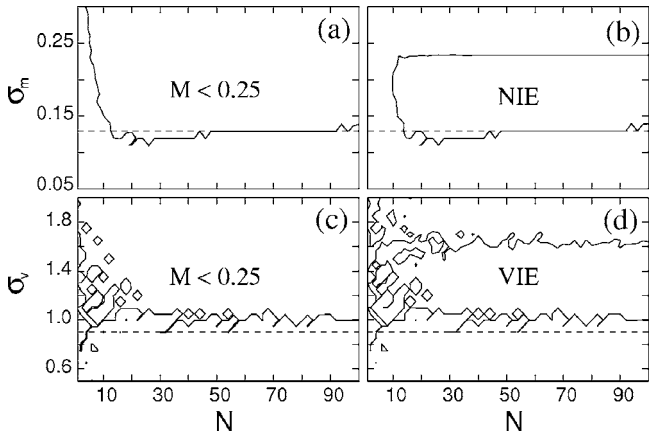

FIG. 6. Results for Eq. (1) with global coupling [Eq. (5)]. (a),(b) boundaries of NIE, $\sigma_v=0$. (c),(d) boundaries of VIE, $\sigma_m=0$. (a),(c) mean field, (—) M_{fi}. (b),(d) relative rest time, (—) RRT_{ex}. (- - -) predicted border oscillatory to excitable net. Other parameters: $q_u=50$.

ences of the noise and to bind the net to the noise induced stable fixed points of the single elements [6]. For a large coupling the transition occurs near the predicted value of σ_m (Fig. 3). The boundaries of the NIE regime are displayed by the RRT. For a large enough coupling an increase of the noise strength starting from $\sigma_m=0$ leads to a jump in this parameter. If the NIE regime is reached a further increase of the noise strength leads to a slow decrease of the RRT. This is due to the fact that growing σ_m now leads to larger fluctuations around the fixed points and to a shift of the stable fixed points to larger values of v_{ij}. This explains, why NIE is found only for a intermediate noise strength.

For a net without noise but in the presence of the variability [Figs. 5(c) and 5(d)] the elements of the net are different from each other and show variable dynamics without coupling. Nevertheless, for coupling strengths $q_u \geq 25$ this large net shows a globally synchronized dynamics (mean field dynamics) for the observed values of the variability strength. In this region of parameter space one finds a transition from an oscillatory to an excitable net, similar to NIE. This variability-induced excitability is found for intermediate variability intensities. For a large coupling the transition occurs near the predicted value of σ_v, but the convergence toward this value is slower than for NIE. This convergence nevertheless confirms the presumption that the dynamics of the net is determined by the parameter $\langle\alpha\rangle$ [Eq. (10)], which is systematically changed by the variability strength (Fig. 3).

In Figs. 6(a) and 6(b) the influence of the net size on the boundaries of the NIE regime is plotted. It is clearly visible that a minimal net size $N\times N$ with $N\approx 10$ is necessary to find NIE. The dynamics of a small net is dominated by the remaining random influences of the noise and hence NIE cannot be observed [6,7]. The larger the net the smaller the remaining random influences of the noise. For a sufficiently by large N the transition occurs at the predicted value of σ_m.

For small N the boundaries of VIE [Figs. 6(c) and 6(d)] are completely different from the boundaries of NIE. In this case no clear contour lines M_{fi} and RRT_{ex} exist and consequently the border of the transition is not well defined. The

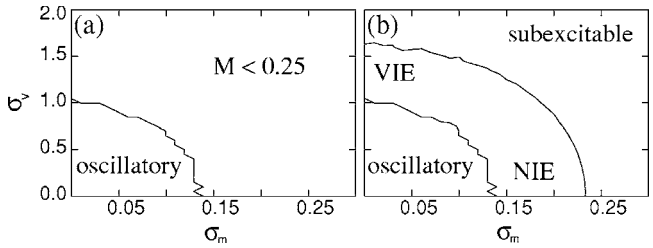

FIG. 7. RRT and M for Eq. (1) with global coupling [Eq. (5)], dependent on σ_m and σ_v. (a) mean field, (—) M_{fi}. (b) Relative rest time, (—) RRT_{ex}. Other parameters: $q_u=50$, $N=100$.

reason for this phenomenon is that the prediction of $\langle\alpha\rangle$ from Eq. (10) is valid only for large N. For small nets $\langle\alpha\rangle$ can differ from the predicted value, and thus the dynamical regime is not completely determined by the variability strength σ_v. For a sufficiently large N the mean gradient angle of the linear nullclines of a net converges toward the prediction and one finds a clear transition from an oscillatory to an excitable net with increasing variability strength. In Fig. 6 such a clear transition is visible for nets with $N\gtrsim 50$.

The results presented show that in large nets with strong coupling the increasing variability strength leads to a clear transition from an oscillatory net to VIE. Knowing the net parameter $\langle\alpha\rangle$ one can predict this transition, which supports the assumption that a systematic effect of the variability is the reason for VIE. This clearly demonstrates, that the transition to a global excitable behavior of the whole net is a collective effect which is not determined by a certain number of excitable elements in an oscillatory net. This assumption is further supported by simulations of a net of FHN elements using additive variability instead of variability in the parameter c. In this case one also gets a fraction of excitable elements depending on the variability strength. Nevertheless the net still shows a more or less disturbed global oscillatory dynamics ($q_u\gtrsim 50$ and $N\gtrsim 100$), even for large variability strengths which lead to a fraction of excitable elements larger then 40%. This can be easily explained using the assumption that $\langle\alpha\rangle$ is relevant for the observed dynamics. Additive variability does not have a systematic effect on the net and thus $\langle\alpha\rangle$ remains unchanged. For that reason one does not find a transition to VIE.

In a next step the combined influence of the noise and the variability in a large net ($N=100$) with a strong coupling ($q_u=50$) is studied. The results are plotted in Fig. 7. The contour line M_{fi} is a function of σ_m and σ_v which corresponds perfectly with the theoretical prediction represented in Fig. 4. This means, that the macroscopic parameter $\langle\alpha\rangle$ determines the dynamics of the observed net. It is not important whether the systematic change of this parameter, which induces the transition, is due to the noise or due to the variability. In Fig. 7(b) the contour line RRT_{ex} divides the parameter space into three distinct areas. For small σ_m and σ_v the net is oscillatory. For parameter values that correspond to the area enclosed by RRT_{ex} the observed net shows excitable dynamics, and for large σ_m and σ_v the net is in the subexcitable regime. The borders between the dynamical regimes correspond qualitatively with the prediction visible in Fig. 4,

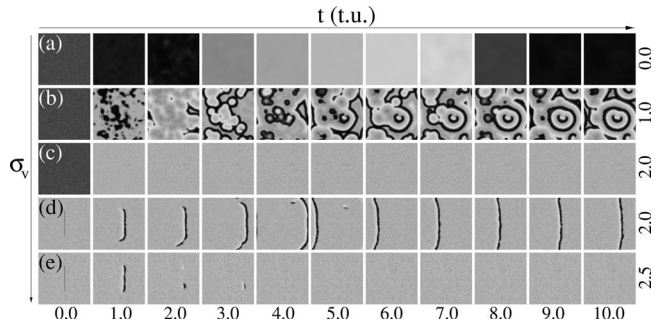

FIG. 8. Snapshots of $u_{ij}(t)$ for Eq. (1) with diffusive coupling [Eq. (6)], dependent on integration time t and σ_v. (a)–(c) Random initial conditions. (d),(e) Initial conditions induce two spiral waves in an excitable net. Other parameters: $N=256$, $q_u=50$, $\sigma_m=0$.

but the border to the subexcitable net is shifted to smaller values of σ_m and σ_v. Nevertheless, these numerical results impressively support the presumption that $\langle\alpha\rangle$ is the relevant parameter for the observed dynamics of a large and strongly coupled net.

In order to study pattern formation and signal transmission through the oscillatory net diffusive coupling [Eq. (6)] is used. Snapshots of the fast variable for different σ_v and $\sigma_m=0$ are plotted in Fig. 8. Looking at Fig. 3(b) a transition to excitability is expected for $\sigma_v \approx 1.0$. For smaller values of the variability strength the net is oscillatory and with appropriate initial conditions a more or less synchronous oscillation results [Fig. 8(a)]. For the predicted value of σ_v the net dynamics changes completely and spiral waves appear. This pattern formation is typical for excitable nets. For larger σ_v [Figs. 8(c) and 8(d)] the spatially uniform, temporally constant solution dominates for almost all initial conditions. Nevertheless excitation waves can still be induced. The border to the subexcitable net, where all excitations die out for $t\to\infty$ [Fig. 8(e)], is found for $\sigma_v=2.1$, nearly the predicted value (Fig. 3). Similar pattern-forming regimes are found for a net with multiplicative noise and $\sigma_v=0$ increasing the noise strength starting from $\sigma_m=0$.

In a next step the interplay of the noise and the variability in a diffusively coupled net is studied (Fig. 9). The borders between the different pattern-forming regimes depend on σ_m and σ_v. For small noise and variability strengths the net is oscillatory and exhibits a nearly synchronous oscillation. The border from the oscillatory to the excitable behavior, where spiral waves appear in the simulation results, follows the prediction from Eq. (10). The transition from pattern formation to a spatially uniform temporally constant behavior is also connected with a certain value of $\langle\alpha\rangle$. The border to the subexcitable regime, which is not visible in Fig. 9, corresponds quite well with the curve $\langle\alpha\rangle=0.260$ in Fig. 4. These results substantiate the assumption that $\langle\alpha\rangle$ is the relevant parameter for pattern formation in the observed net. One just has to know the value of $\langle\alpha\rangle$ to predict the patterns found in the simulations.

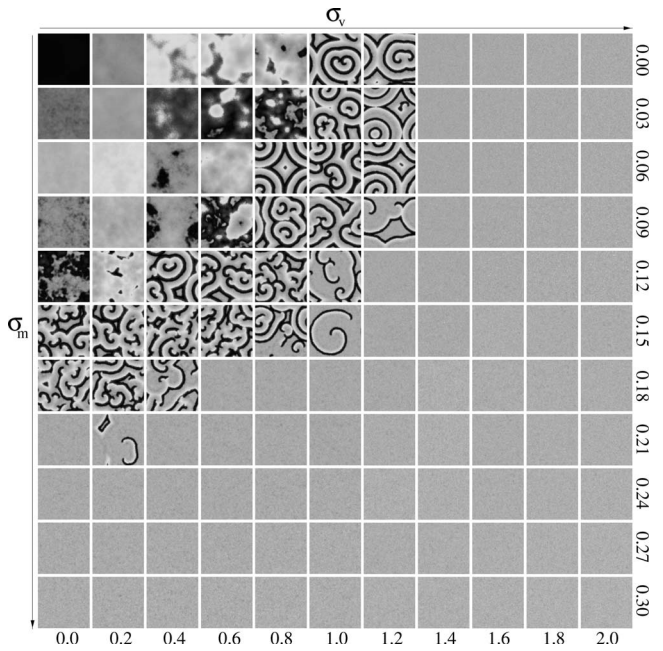

FIG. 9. Snapshots of $u_{ij}(t)$ for Eq. (1) with diffusive coupling [Eq. (6)] and random initial conditions, dependent on σ_v and σ_m. Other parameters: $t=50$ t.u., $N=256$, $q_u=50$.

In summary, it has been shown that variability can induce a transition to excitability in a large oscillatory net of neural elements with a strong coupling. This transition is explained by a systematic effect of the variability, which changes the macroscopic net parameter. A theoretical expression for this parameter, in dependence on the variability strength, provides a prediction of the border to VIE in the limit of large N and strong coupling.

In a net with additional multiplicative noise the parameter $\langle\alpha\rangle$ depends on the noise strength as well and so does the border of the described transition. Simulations of the net show the transition for the expected values of σ_m and σ_v. This substantiates the fact that the parameter $\langle\alpha\rangle$ determines the dynamics of the observed net. The transition to excitability implies the ability of a diffusively coupled net to show pattern formation. In simulations the expected patterns are found in the predicted regions of parameter space. Thus the parameter $\langle\alpha\rangle$ determines the patterns found in the simulated net.

The transition to excitability was studied using the paradigmatic FHN model in a rather general framework. We hope that these theoretical findings will contribute to the theory of extended systems influenced by variability and noise [4]. Maybe our results can also help to develop new strategies to suppress malfunctioning neural oscillations and to restore the functionality of neural networks.

[1] L. Gammaitoni, P. Hänggi, P. Jung, and F. Marchesoni, Rev. Mod. Phys. **70**, 223 (1998).
[2] P. Jung and G. Mayer-Kress, Phys. Rev. Lett. **74**, 2130 (1995).
[3] H. Busch and F. Kaiser, Phys. Rev. E **67**, 041105 (2003).
[4] J. García-Ojalvo and J. M. Sancho, *Noise in Spatially Extended Systems* (Springer, Berlin, 1999).
[5] J. S. Nagumo and S. Yoshizawa, Proc. IRE **50**, 2061 (1962).
[6] E. Ullner, A. Zaikin, J. García-Ojalvo, and J. Kurths, Phys. Rev. Lett. **91**, 180601 (2003).
[7] E. Glatt, H. Busch, F. Kaiser, and A. Zaikin, Phys. Rev. E **73**, 026216 (2006).
[8] A. T. Winfree, J. Theor. Biol. **16**, 15 (1967).
[9] Y. Kuramoto, *Chemical Oscillations, Waves and Turbulence* (Springer, Berlin, 1984).
[10] A. Pikovsky, M. Rosenblum, and J. Kurths, *Synchronization. A Universal Concept in Nonlinear Sciences* (Cambridge University Press, Cambridge, U.K., 2001).
[11] Y. Braiman, J. F. Lindner, and W. L. Ditto, Nature (London) **378**, 465 (1995).
[12] M.-T. Hütt, H. Busch, and F. Kaiser, Nova Acta Leopold. **332**, 381 (2003).
[13] M. Kaern, T. C. E. W. J. Blake, and J. J. Collins, Nat. Rev. Genetics **6**, 451 (2005).
[14] J. K. Douglass, L. Wilkens, E. Pantazelou, and F. Moss, Nature (London) **365**, 337 (1993).
[15] D. F. Russell, L. A. Wilkens, and F. Moss, Nature (London) **402**, 291 (1999).
[16] S. Kádár, J. Wangi, and K. Showalter, Nature (London) **391**, 770 (1998).
[17] S. Alonso, I. Sendina-Nadal, V. Perez-Munuzuri, J. M. Sancho, and F. Sagues, Phys. Rev. Lett. **87**, 078302 (2001).
[18] J. Moehlis, J. Math. Biol. **52**, 141 (2006).
[19] A. T. Winfree, *When Time Breaks Down: The Three-Dimensional Dynamics Of Electrochemical Waves and Cardiac Arrhythmias* (Princeton University Press, Princeton, NJ, 1987).
[20] P. Jung, A. Cornell-Bell, F. Moss, S. Kadar, J. Wang, and K. Showalter, Chaos **8**, 567 (1998).